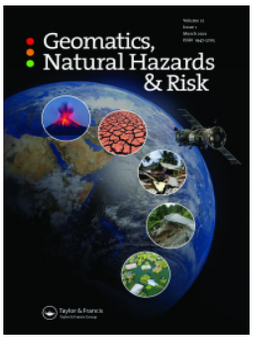

Geomatics, Natural Hazards and Risk

ISSN: (Print) (Online) Journal homepage: www.tandfonline.com/journals/tgnh20

Deep geophysical investigations (DERT and Seismic Reflection) to unravel the Ferrara urban area geology

Enzo Rizzo, Riccardo Caputo, Lorenzo Petronio, Valeria Giampaolo, Luigi Capozzoli, Gregory De Martino, Sabatino Piscitelli, Jessica Bellanova, Dimitra Rapti, Luca Baradello, Alessandro Affatato & Vincenzo Lapenna

To cite this article: Enzo Rizzo, Riccardo Caputo, Lorenzo Petronio, Valeria Giampaolo, Luigi Capozzoli, Gregory De Martino, Sabatino Piscitelli, Jessica Bellanova, Dimitra Rapti, Luca Baradello, Alessandro Affatato & Vincenzo Lapenna (2024) Deep geophysical investigations (DERT and Seismic Reflection) to unravel the Ferrara urban area geology, Geomatics, Natural Hazards and Risk, 15:1, 2423748, DOI: 10.1080/19475705.2024.2423748

To link to this article: https://doi.org/10.1080/19475705.2024.2423748

© 2024 The Author(s). Published by Informa UK Limited, trading as Taylor & Francis Group.

Published online: 03 Nov 2024.

Submit your article to this journal

View related articles

View Crossmark data

Full Terms & Conditions of access and use can be found at
https://www.tandfonline.com/action/journalInformation?journalCode=tgnh20

GEOMATICS, NATURAL HAZARDS AND RISK
2024, VOL. 15, NO. 1, 2423748
https://doi.org/10.1080/19475705.2024.2423748

Taylor & Francis
Taylor & Francis Group

OPEN ACCESS Check for updates

Deep geophysical investigations (DERT and Seismic Reflection) to unravel the Ferrara urban area geology

Enzo Rizzo[a,b], Riccardo Caputo[a], Lorenzo Petronio[c], Valeria Giampaolo[b], Luigi Capozzoli[b], Gregory De Martino[b], Sabatino Piscitelli[b], Jessica Bellanova[b], Dimitra Rapti[d], Luca Baradello[c], Alessandro Affatato[c] and Vincenzo Lapenna[b]

[a]Department of Physics and Earth Sciences, Ferrara University, Ferrara, Italy; [b]National Research Council, Institute of Methodology for Environmental Analysis (CNR-IMAA), Italy; [c]National Institute of Oceanography and Applied Geophysics (OGS), Trieste, Italy; [d]Department of Chemical, Pharmaceutical and Agricultural Sciences, University of Ferrara, Ferrara, Italy

ABSTRACT

Exploring the 'fragile crust of our planet' is crucial for human survival holding an immense social and economic significance. Therefore, innovative approaches become of utmost importance for obtaining precise subsoil models in urban areas making the latter more resilient to natural disasters. Due to logistic issues and a high level of anthropogenic disturbance and related background noise, urban areas are usually intrinsically more problematic for applying geophysical prospecting methods. This work presents the results obtained by Deep Electrical Resistivity Tomography and P wave Seismic Reflection surveys performed along the Ferrara, north Italy, city walls documenting the adaptability of the geophysical surveys and how it is possible to obtain high-quality electrical resistivity and seismic data even in complex urban settings. The joint interpretation of geoelectrical and seismic data fully integrated with tectonic, geological and hydrogeological information allowed to reconstruct the stratigraphic evolution down to a depth of about 1.5 km. These results highlight the occurrence of a syndepositional Quaternary tectonic tilting associated with the growth of a fault-propagation fold.

ARTICLE HISTORY
Received 28 July 2024
Accepted 26 October 2024

KEYWORDS
Deep electrical resistivity tomography; seismic reflection; urban geophysics; hydrogeology; urban geology

1. Introduction

The urban population of the world has grown rapidly since 1950, having in-creased from 751 million to 4.2 billion in 2018 (United Nations 2019). Growth of urban density is driven by both the overall population trend and the progressive movements towards urban areas. These two factors are projected to add 2.5 billion to the world's urban population by 2050, with almost 90% of this growth occurring in Asia and

CONTACT Enzo Rizzo enzo.rizzo@unife.it Department of Physics and Earth Sciences, Ferrara University, Ferrara, Italy; National Research Council, Institute of Methodology for Environmental Analysis (CNR-IMAA), Italy

© 2024 The Author(s). Published by Informa UK Limited, trading as Taylor & Francis Group.
This is an Open Access article distributed under the terms of the Creative Commons Attribution License (http://creativecommons.org/licenses/by/4.0/), which permits unrestricted use, distribution, and reproduction in any medium, provided the original work is properly cited. The terms on which this article has been published allow the posting of the Accepted Manuscript in a repository by the author(s) or with their consent.

Africa. Therefore, urban areas are expected to absorb virtually all of the future growth of the world's population. On the other hand, forecasts based on the best available scientific evidence indicate that in the coming decades, climate change may induce hundreds of millions of urban residents increasingly vulnerable to floods, landslides, extreme weather events, and other natural disasters (United Nations 2020). Accordingly, this rapid evolution poses challenges for the set-up of an ambitious urban development agenda that seeks to make cities and human settlements inclusive, safe, resilient and sustainable (SDG 11). For example, it is worth to note that 90% of all reported COVID-19 cases occurred within urban areas which became epicenters for the pandemic diffusion. As a result, cities are increasingly compelled to address the reality that unplanned urbanization can lead to conditions where many residents lack adequate access to water and sanitation facilities, particularly in overcrowded areas where physical distancing is difficult (United Nations 2020). To tackle these challenges, it is essential to adopt new strategies and programs for planning new urban centres or expanding existing ones. Such initiatives should aim to enhance resilience to natural disasters and health emergencies, while also improving groundwater resources and promoting energy and environmental sustainability. These plans require a good knowledge of the subsoil which, due to its complexity, in urban and logistic terms, makes classical diagnostics inappropriate for the purposes.

The city of Ferrara, Northern Italy (Figure 1), was thus selected as a test site in the frame of the CLARA (CLoud plAtform and smart underground imaging for natural Risk Assessment) project being affected by both hydraulic, hydrogeologic, seismic, and environmental risks. The scientific and technological challenge of the project consists in developing from a Smart Cities perspective, innovative products and services for the mitigation of the above risks in urban and suburban areas through the active involvement of Public Administrations (Castelli et al. 2019).

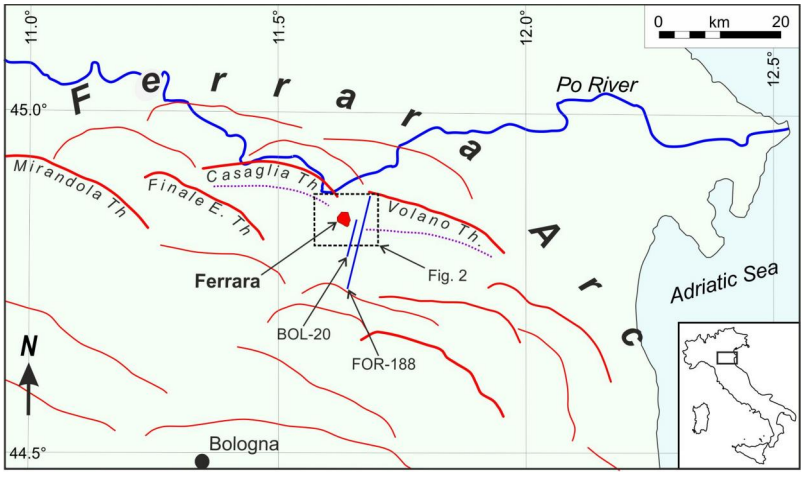

Figure 1. Simplified tectonic map of the Eastern Po Plain showing the projected traces (red curves) of the major fault segments belonging to the Ferrara Arc. Dotted curves indicate the crest of the anticlines associated to the Casaglia and Volano thrusts. Blue lines represent the traces of the deep seismic reflection profiles. See inset map for location.

Currently, there is a pressing need to develop innovative approaches for creating detailed geological models of the subsoil in urban areas. Geological mapping in densely populated regions presents significant challenges due to the scarcity of suitable outcrops that can inform our understanding of subsurface conditions. Additionally, drilling boreholes for direct observations can be expensive, and urban layouts often limit the optimal placement of wells due to logistical constraints. In areas of particularly complex geology, this scattered information is commonly not enough to provide a detailed picture of the shallow subsurface (Martí and Carbonell 2016). On the contrary, the geophysical exploration of the subsoil in a dense urban environment (where there is generally an intrinsic difficulty to perform direct surveys and invasive drillings) could potentially respond to this expectation. Notwithstanding, the highly anthropogenically modified setting, the presence of several infrastructures and underground utilities can strongly affect also this kind of sub-soil exploration.

The role of applied geophysical techniques in addressing the challenges of increasing global urbanization is set to expand significantly. In this context, a comprehensive understanding of the geological subsoil, the lithostratigraphic distribution and the hydrogeological model, and its interaction with urban infrastructures becomes essential for effective urban planning at any foundational level. A novel sub-discipline, called Urban Geophysics (Liu and Chan 2007; Lapenna 2017) has been recently developing in the field of geophysics for analysing limits and potentialities of well-known geophysical techniques in urban and industrialized areas. Urban geophysics aims to simplify and streamline the planning phase by providing a large amount of information readily available for consultation by designers and competent bodies in public administration. This includes detailed information about the geological subsurface. In order to increase the geological knowledge in the urban context, it is possible to apply different geophysical methods. Their remote sensing ability offers several advantages compared with other invasive methods like drilling or penetrometer tests. The most appropriate methods are Ground Penetrating Radar (GPR), Electrical Resistivity Tomography (ERT), electromagnetic (EM), seismic (S) and micro gravity (mG) techniques. The choice of the more proper methodologies to be applied depends on the purpose of the prospecting and, in particular, by the contrasts between the geophysical properties in the subsoil lithologies or sediments, the required depth of investigation, the logistics for the deployment of the sensors and the economic feasibility. At this regard, the urban environment poses significant challenges for geophysical studies due to elevated levels of ambient noise, impacting the accuracy of data collection, and on the applicability of the different geophysical prospecting methods. Therefore, mitigating background noise in geophysics can be achieved through advanced signal processing techniques, strategic site selection, and the implementation of noise reduction technologies, enhancing the precision and reliability of data acquisition. In shallower applications, GPR and ERT have been used for exploring the shallower layers of the urban subsurface, with resolution from tens of centimetres to tens of metres, for the detection and geometric characterization of buried ancient structures, anthropogenic and lithological-structural features, buried cavities and archaeological remains (Papadopoulos et al. 2009; Rizzo et al. 2019b; Bellanova et al. 2020; Capozzoli et al. 2023). Moreover, passive and active seismic approaches could provide further

contributions to the development of a reliable geological model of the investigated area and feed numerical procedures devoted to the assessment of seismic response (Calamita et al. 2019; Tragni et al. 2021; Gangone et al. 2023).

Among the several geophysical techniques, seismic reflection can provide the appropriate penetration depth and resolution for achieving a relatively detailed geological interpretation of the subsoil providing 2D and even 3D imaging thus enabling, for example, the recognition of fractures networks, the reconstruction of the fault geometry or other deformational structures, and generally of the overall stratigraphy. Besides the expected development related to oil and gas exploration companies, the increasing interest in shallow subsurface has provided a completely new insight to seismic methods, mainly related to instrumentation and processing techniques to obtain higher vertical and horizontal resolution and to overcome the challenges of the complex upper part of the subsurface in unconventional environments and applications. Therefore, the right planning of the acquisition experiment is essential to ensure the success of a seismic survey in an urban environment (Liu and Chan 2007). Several seismic surveys were performed in urban settings by using frequency-controlled vibriosis sources both in P- and SH-waves. As an example, Liberty (2011) acquired five reflection seismic profiles in residential streets to identify and characterize potentially active faults that cross the downtown Reno city, Nevada area.

On the other hand, deep applications of electromagnetic geophysical methods in urban areas are very uncommon. A rare example is represented by Gabàs et al. (2014) which combined the controlled source audio-magneto-telluric method (CSAMT), the magneto-telluric method (MT), the microtremor H/V analysis, and the ambient noise array measurements for mapping the bedrock depth and constraining the thickness of Quaternary sediments in the broader Girona and Salt areas (NE of Spain). In the research proposed by Rapti-Caputo et al. (2009), the conceptual hydrogeological and hydrochemical model, based on direct drilling data, up to a depth of 500 m, was integrated by a detailed and repeated 3D resistivity investigation using combined ERT, Time-Domain Electromagnetic Soundings (TDEM) and in-hole measurements of the geoelectrical parameters. More recently, Carrier et al. (2019) acquired reflection seismic profiles, gravimetric data, and a 4.5 km-long 2-D deep geoelectrical survey at the edge of the industrial area of Satigny (North of Geneva, Switzerland) to investigate the subsurface down to 1.5 km-depth for geothermal exploration.

The Deep Electrical Resistivity Tomography (DERT) method was introduced by Perez Flores and Treviño (1997). They studied the Ahuachapan-Chipilapa geothermal field (El Salvador), where four resistivity profiles were carried out with electrode distances between 500 and 100 m for detecting the geometry of conductive zones associated with the presence of geothermal fluids. Although the long time since its proposal, DERT applications are not widespread in general, and indeed few examples have been published so far (Di Maio et al. 1998; Storz et al. 2000; Suzuki et al. 2000; Colella et al. 2004; Rizzo et al. 2004, 2019c, 2022; Giocoli et al. 2008; Pucci et al. 2016; Rizzo and Giampaolo 2019; Troiano et al. 2019, Sapia et al. 2021; Balasco et al. 2022; Olita et al. 2023). All pre-existing DERT applications are associated with geological, hydrogeological and geothermal investigations in extra urban areas highlighting the feasibility of the technique both from the logistic and instrumental aspects, in

addition to that of signal analysis. At this regard, this technique represents a good approach in areas where it is important to study the presence and the circulation of fluids, such as in areas of geothermal interest. Indeed, within or close to urbanized areas, the direct use of the geothermal resources could be very fruitful due to the short connection to the district heating network. A critical point when using electrical resistivity techniques in urbanized areas is represented by the commonly high level of electric noise. Accordingly, the DERT technique represents a real challenge for its operating mode in urban settings where the major critical points could be logistics, instrumental and data analysis methods for the noise removal (Balasco et al. 2022).

Within the urban area of Ferrara, a 5500 m-long DERT and a 2500 m-long P-waves seismic reflection profile were selected for carrying out two different geophysical methods along the same path (Rizzo et al. 2019a; Figure 2). The aim of this double geophysical investigation was to improve the geological information in correspondence of an urban context. We also performed a joint interpretation of DERT and seismic data which certainly represent an important added value to the research.

The city of Ferrara stands on the eastern sector of the Po Plain (Figure 1), a morphologically flat region, and covers an area of about 404 km^2 with a population of about 132.000 inhabitants. It was founded in the early Middle Ages, as a small castrum on the natural bank of the Po River and then progressively expanded, initially in a linear way along the riverbank, then with subsequent additions in Renaissance times, made possible by hydraulic reclamation works and the migration of the riverbanks (Patitucci Uggeri 1989; Uggeri 1989; Cremaschi and

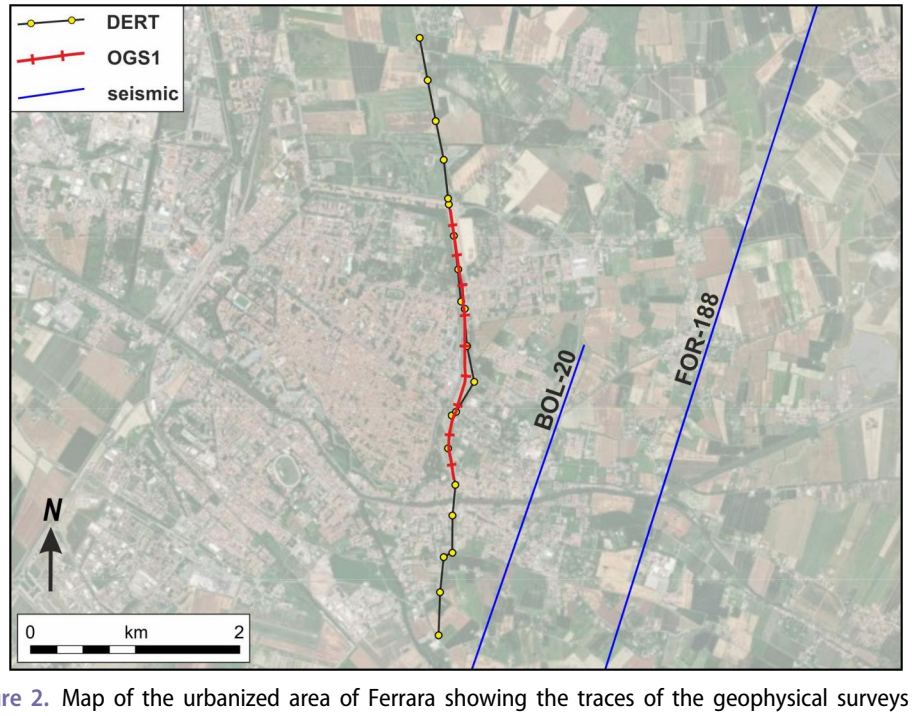

Figure 2. Map of the urbanized area of Ferrara showing the traces of the geophysical surveys carried out in the frame of the present research (black and red curves) and the two deep seismic reflection profiles used for comparison (blue lines). See Figure 1 for location.

Nicosia 2010). The various parts of the city, settled in successive phases, have different geological characteristics and are subjected to different levels of environmental risks, among which those associated with flooding and potential river routes of the Po or Reno rivers, that probably will be exacerbated in the future by climate change. Moreover, an important historical seismicity (Guidoboni 1984; Caputo et al. 2016), significant seismic amplification factors and a high liquefaction potential also characterize the studied area.

The hydrogeological setting of the city area and its surroundings has been largely investigated by means of numerous drinking water wells and exploratory boreholes (generally <150 m), and penetrometer logs (generally <35 m), therefore providing direct and indirect information for the shallow subsoil. However, deep geological and geophysical data (e.g. deep bore-holes stratigraphy, geological-structural studies, seismic reflection profiles as well as active and passive site measurements) are available only outside Ferrara, where investigations were extensively carried out in the past decades mainly for hydrocarbon exploration purposes. Consequently, deep geological and structural knowledge in correspondence of the volume underlying the broader urbanized area of Ferrara is completely lacking.

2. Tectonic, stratigraphic and hydrogeological framework

The investigated area belongs to the eastern sector of the Po Valley, which represents a morphologically flat alluvial plain since most of the Quaternary. The uppermost continental sedimentary succession covers, and it is partly slightly deformed by, a series of underlying tectonic structures forming the so-called Ferrara Arc (Pieri and Groppi 1981; Bigi et al. 1992) belonging to the Neogene-Quaternary Northern Apennines fold-and thrust belt (Figure 1). In particular, this second-order arc (Caputo and Tarabusi 2016) corresponds to the frontal most portion of the continental accretionary wedge and consists of a complex thrust system composed of several interconnected minor segments, commonly 10-30 km-long and characterized by different degrees of overstepping and overlapping geometries (Pieri and Groppi 1981; Bigi et al. 1992).

Inherited crustal features have likely contributed to this structural complexity, both in space and time. Faulting along the Ferrara Arc is typically blind (Figure 2). Most of these tectonic structures are seismogenic and capable of producing at least moderate earthquakes (i.e. $M = 5$-6); in case of co-seismic linkage with nearby segment(s), the occurrence of stronger events could be not ruled out, possibly up to $M = 6.5$. For example, two of these segments (Mirandola and Finale Emilia thrusts; Figure 1) were the causative faults of the 2012 Emilia seismic sequence (Pezzo et al. 2013; Bonini et al. 2014; Govoni et al. 2014; Vannoli et al. 2015).

Several available seismic reflection profiles and deep wells for hydrocarbon exploration (e.g. Pieri and Groppi 1981; Regione Emilia-Romagna & ENI-AGIP, 1998; Toscani et al. 2009) document that the Mesozoic-Lower Tertiary, mainly carbonate, succession is strongly affected by thrusting characterized by prevailingly low-to-medium dip-angle surfaces, showing large displacements locally up to some kilometres (Figure 2). Moreover, the Tertiary and Quaternary, essentially

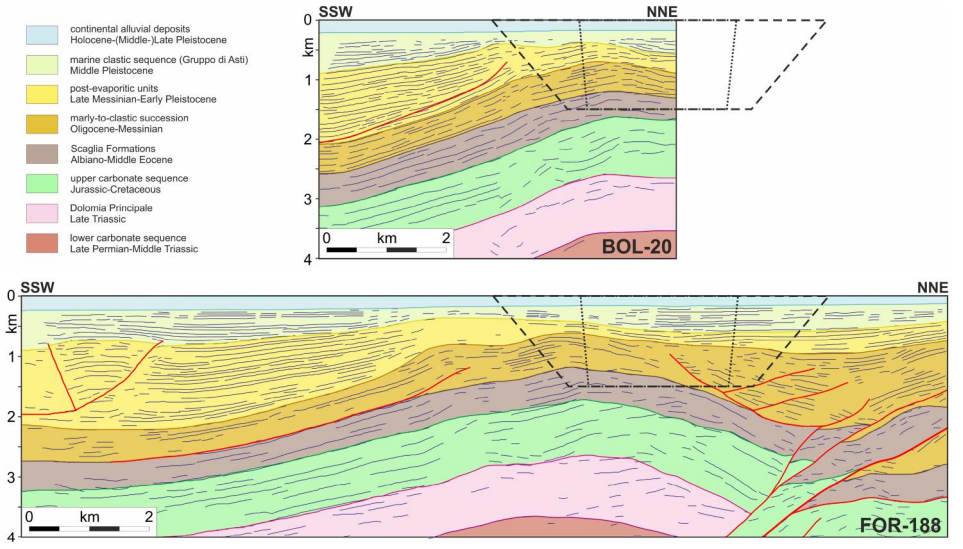

Figure 3. Interpreted seismic reflection profiles east of Ferrara (modified from [48]) showing the projection of the OGS1 (dotted line) and DERT (dashed line) geophysical surveys carried out in the present research. Traces are represented in Figure 1.

clastic, sedimentary succession is largely involved in the deformation with a dominant vergence towards the north.

Associated with the fault system, large-scale folds commonly develop as ramp anticlines (fault-related folds) or as fault-propagation folds (Figure 3), but also other secondary accommodation structures could form in correspondence of some segment boundaries separating thrusts with different settings and kinematics. It is worth to note that Ferrara stands on top of such transfer structure geometrically and kinematically connecting the Casaglia Thrust with the Volano Thrust (Figure 1), which form a left-lateral overstepping (and underlapping?) geometry. The geophysical investigations carried out in the present research will also contribute to shed some light on this issue.

As above mentioned, late Neogene-Quaternary tectonics is basically synsedimentary as clearly documented by the strong lateral thickness variations, pinch-out geometries and overlap settings as well as fan shape layering in association with growth synclines. Similarly, inferred sedimentation rates are characterized by a high lateral variability from almost zero, or even erosion, to several mm/a (e.g. Ghielmi et al. 2013; Mastella 2018; Amorosi et al. 2021; Severi 2021). Notwithstanding the positive vertical movements locally occurring in correspondence with the anticlines, the broader Po Plain is dominated by a regional scale subsidence (e.g. Caputo et al. 1970; Arca & Beretta, 1985; Carminati et al. 2003; Cenni et al. 2013). Accordingly, accommodation space is continuously generated, sedimentation follows, and progressively buries the growing tectonic structures (both faults and folds). As a further consequence of this persistent competition between tectonics and sedimentation, the depth of the carbonate bedrock varies between several kilometres in the synclines and few hundred metres at the crest of the anticlines, while as a first approximation, topography remains roughly flat across the entire area (e.g. Bigi et al. 1992).

Based on seismic reflection profiles and deep boreholes carried out for hydrocarbon explorations some decades ago, it is possible to reconstruct the subsoil geology down to several km-depth (Figure 3) thus allowing to recognize of the occurrence, the position and the geometry of the major tectonic structures affecting the area. In the frame of a collaboration with ENI SpA, we could analyse numerous seismic profiles (Valenti 2015; Allegra Garufi, 2016; Mistroni 2016; Mastella 2018; Rapti and Caputo 2021) allowing us to acquire a general picture of the regional tectonics including the area investigated in the present paper.

For the goals of the present note, we will focus on two of the analysed profiles, referred to as BOL-20 and FOR-188, being the closest ones to the town of Ferrara (Figure 1). The traces of the selected profiles are parallel and oriented NNE-SSW, running at ca. 0.5-–1.0 and 1.5–3.0 km east, respectively, of the Ferrara Renaissance walls, therefore in a direction almost parallel to that of our roughly N-S geophysical surveys (Figure 2). Both profiles clearly confirm the presence of a ramp-anticline oriented ESE-WNW whose crest runs close to the southeastern corner of the city walls. This tectonic structure, here referred to as the Volano Thrust (or anticline; Figure 1), continues ESE-wards for more than 20 km with a slightly curved shape in plan view. At a depth of 5-6 km, the available seismic profiles show that this fault is characterized by a partitioning of the displacement branching up-dip and forming some major splays affecting the whole Tertiary succession (Mastella 2018). Seismic reflection profiles clearly show that the whole sedimentary succession from Triassic to Pleistocene has been involved in the shortening.

Also west of Ferrara, the shallow crustal volume is affected by a similar tectonic structure, which has been however much more investigated because it contains a medium enthalpy geothermal reservoir exploited since decades to support the district heating network serving a large portion of the Ferrara buildings. It is the Casaglia Thrust mainly trending E-W and turning to an ESE-WNW direction in its eastern sector (Figure 1). It is ca. 22 km-long and characterized by a well-defined ramp that accommodates most of the shortening thus describing a different deformational style with respect to the Volano Thrust in terms of geometry, setting and position of the ramp and the presence of secondary accommodation structures lacking in the eastern structure investigated by our geophysical surveys.

Although both belonging to the broader Ferrara Arc, the two structures had clearly distinct and different geometric, kinematic, and probably chronological evolutions, thus representing potential fourth-order seismogenic sources (*sensu* Caputo and Tarabusi 2016). As a further consequence, in correspondence to Ferrara there likely exists a hard segment boundary somehow linking the two major tectonic elements. Lacking deep industrial seismic profiles within the urbanized area, the present research could also contribute to shed some light on this issue.

The infilling of the Po Basin displays an overall regressive tendency, from Pliocene open marine to Quaternary marginal marine and then alluvial deposits, corresponding to the marine (Qm; age $>$ 0.65 Ma) and continental Quaternary (Qc; commonly referred to as the 'Emilia-Romagna Supersynthem') stratigraphic cycles (Ricci Lucchi et al. 1982). The large-scale architecture is characterized by an internal subdivision of the succession into several unconformity-bounded

stratigraphic units (UBSU), where each unconformity represents a phase of basin re-organization (Amorosi et al. 2008).

The ca. 0.45 Ma unconformity of tectonic origin (Regione Lombardia and ENI-AGIP; 2002), allows to subdivide the 'Emilia-Romagna Supersynthem' into two lower-rank ones: 'Lower Emilia-Romagna Synthem' (AEI) and 'Upper Emilia-Romagna Synthem' (AES) being the latter strongly influenced by the Milankovitch-scale (ca. 100 ka) cyclicity (Amorosi et al. 2008).

From a hydrogeological point of view, within AES, AEI and the underlying deposits are developed three major Aquifer Groups, referred to as *A*, *B* and *C* further subdivided into aquifer systems. Up to a depth of 500 m within the study area, group *A* includes four major aquifer systems (*A1* to *A4*), similar to group *B* (*B1* to *B4*), while group *C* includes five major aquifer systems (*C1* to *C5*) in reality poorly explored (Regione Emilia-Romagna & ENI-AGIP, 1998; Rapti-Caputo et al., 2000; Molinari et al. 2007). The aquifers in groups *A* and *B* are mainly developed in alluvial deposits and particularly within the coarse-grain component of the alluvial fans and in the sandy layers associated to the Po River channels. On the other hand, the aquifers of group C mainly consist of coastal and marine marginal deposits, characterized by sands alternating with finer sediments.

The geometrical parameters (thickness and lateral distribution) and the geochemical and hydrodynamic characteristics of the aquifers strongly depend on the lateral and vertical facies variations of the sedimentary successions, which in turn are governed by the tectonic activity and the continuously varying depositional environments (continental, lacustrine or marine, e.g. Rapti-Caputo et al., 2000).

Consequently, the Pliocene-Quaternary deposits in the subsoil of the investigated area are characterized by silty-muddy layers alternating with sandy and sometimes gravel lenses. In particular, within the first 500 m in correspondence of the broader Ferrara area, it is possible to distinguish three main aquifers groups *A*, *B,* and *C* (Regione Emilia-Romagna & ENI-AGIP, 1998; Rapti Caputo 2000), where the confined aquifers consist of sandy layers with variable grain size or sandy-silt material. These aquifers are in general hydraulically separated by layers with low permeability (mainly silt or clay-silt). It should be noted that (Figure 4), firstly, Group *A* is in general saturated in fresh water with a total thickness of about 150 m, though the aquifer system A_4 is locally absent. Secondly, in the investigated area the top of Group *B* occurs at a depth of 150 m with a thickness of about 70 m and it is saturated with fresh water. On the contrary, the lower portion of *B*, between 220 to ca. 550 m, is saturated with salt/brackish water. Thirdly, all deeper aquifers belonging to Group *C* obviously contain salty water.

3. Geophysical data and methods

As above mentioned, the CLARA project was devoted to applying 'deep' geophysical prospecting methodologies to urban settings, and to achieve this target we carried out seismic reflection and 2D Deep Electrical Resistivity Tomography (DERT) campaigns in the city of Ferrara allowing to investigate as deep as ca. 1500 m below the ground surface. The deep geophysical surveys were conducted along the vallum between the

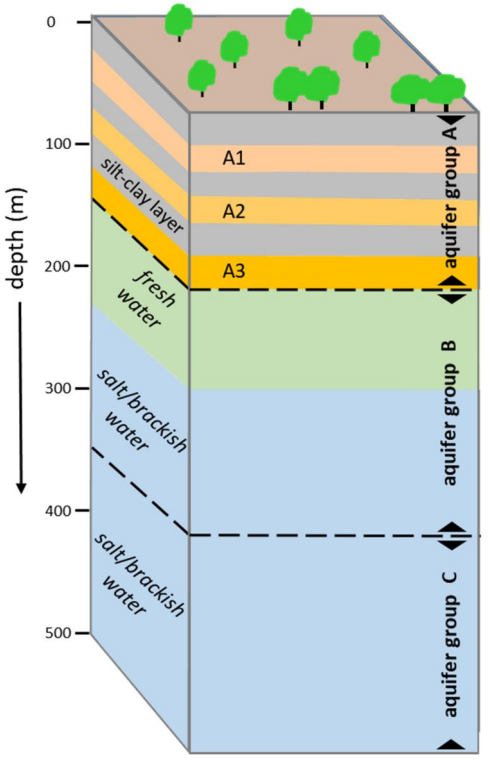

Figure 4. Simplified hydrogeological framework in correspondence of the Eastern Ferrara sector showing a greater detail in the first 150 m, where *A1*, *A2* and *A3* aquifers have been distinguished.

sixteenth-century walls and the modern eastern sector of the town. In particular, a seismic reflection line (2630 m-long) was acquired along the currently dry moat (Figure 2). Due to the intense vehicular transit and the multiple anthropogenic activities that could condition the seismic acquisition, the survey was carried out at night, with partial closure to the circulation of some road sections, thanks to the collaboration of the Ferrara Administration. This allowed to largely improve the quality of the collected data.

A DERT profile (5600 m-long) partially superimposed on the seismic profile was also performed (Figure 2). The geoelectric survey was conducted during the day. In order to prevent the crossing of the cables from any road and therefore avoid the necessary closure of road traffic, electrodes were installed on vegetated surfaces both in private and public gardens. We wish to remind that managing geophysical surveys in an urban environment is challenging in terms of work organization, timing and site safety, as well as to reduce any possible act of vandalism. Permits for working in public areas and for accessing private ones were provided and facilitated by a municipal ordinance.

3.1. Seismic reflection profile

Seismic reflection is a geophysical method that provides information about the subsurface structures of the ground (e.g. Yilmaz 2001). In this method, acoustic waves

are sent into the ground, which are reflected from the various buried structures (Sato et al. 2012). The signal recorded by geophones at the surface is proportional to impedance contrasts (the product of density and seismic velocity). In general, geophysical surveys are divided into shallow and deep surveys. The methods mainly differ in a) the energy sources, b) the geometry of the source and the receivers (<5 m distance between receivers for shallow reflections, 5-60 m for deep reflections) and c) the type of used receivers (low-frequency geophones for deep, high-frequency geophones for shallow reflections; (Steeples 1998). For shallow seismic surveys, sledgehammers, portable vibrators and mechanical weight drops are most commonly used, while vibroseis and explosives are used for deep seismic surveys. In the frame of this project, we therefore recorded a reflection seismic line with a MiniVib source in P-wave mode.

The seismic survey was carried out using a DMT Summit II telemetry system equipped with a 24-bit A/D sigma-delta converter. A MiniVib T-2500 was used as the acoustic source. The vibration source was instead selected as a pulse source because it is possible to apply the same energy at a lower intensity over a longer period (Laing 1972, 1989; Goupillaud 1974). Low intensity is always required when the seismic survey is close to buildings or archaeological remains as was the case for this survey (Figure 5a).

Arrays of 6 geophones (10 Hz) with a pattern spacing of 10 m were used as receivers to attenuate the ground-roll effect (Morse and Hildebrandt 1989) and random noise (Savit et al. 1958). We performed FSW and FRW tests (Vincent et al. 2006), in which we determined near-surface seismic phase velocities for different coherent wave trains. The tests show that an upsweep in the frequency range between 8 and 140 Hz propagating linearly in 16 sec had a satisfactory penetration into the ground with a force of 2500 lb. To limit the ripple effects in the clapper, a 10% taper was applied. The energization point was selected every two stations (i.e. 20 m), and two or more shots were conducted at each point. The entire line was covered with a fixed distribution of 264 stations. All seismic parameters are reported in Table 1.

After data collection and before data processing, it was necessary to check the data quality (QC) in the pre-processing phase. The field data were recorded without correlation. Cross-correlation with the sweep pilot was performed after a predictive deconvolution was applied to the uncorrelated data to reduce environmental noise (Baradello and Accaino 2013). After verifying the survey geometry, the entire seismic dataset was edited shot-by-shot to remove noisy traces and then the energizations performed at the same position were merged (vertical stack). The basic processing steps to increase and improve the signal-to-noise ratio were, firstly, an amplitude recovery (geometric divergence and ground absorption), and secondly, an attenuation of the coherence noise (ground roll) using a trimmed mean dynamic dip filter and bandpass filtering. Zero-phase deconvolution was successfully performed to increase the vertical resolution (Berkhout 1977). Semblance and CSV algorithms were applied to groups of common deep points (super gathers) to calculate the seismic velocity across the sediments. The seismic velocity information led to the time correction of the reflections (normal move-out) in the individual CDP before stacking. The final result of the stacked section (in the following referred to as OGS1) shows several

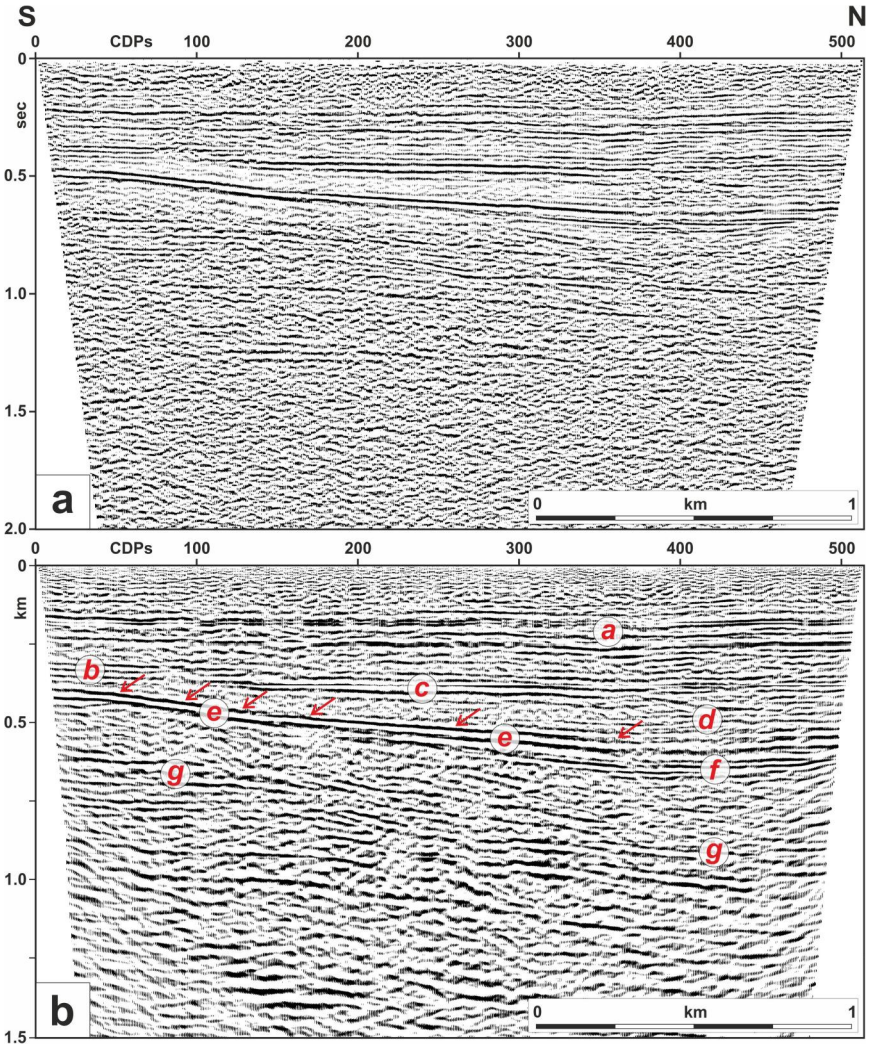

Figure 5. a) Seismic reflection profile OGS1 acquired within the Eastern sector of the Ferrara urbanized area. b) Same profile depth converted using the smoothed interval velocity field, calculated from stack velocity with Dix (the indicated labels are described in the main text). See Figure 2 for location.

Table 1. Values of the principal parameters used during the seismic reflection survey.

Record windows	19 s
sweep length	16 s
sampling rate	2 ms
frequency range	8-140 Hz

non-horizontal subsurface structures (Figure 4) so a Kirchhoff time migration was required. To convert the section in the depth domain, we used the interval velocity calculated with Dix from the stack velocity table (Yilmaz 2001).

3.2. Deep electrical resistivity tomography

The basic principle of the geoelectrical method is to inject a current, I (expressed in A), into the earth by using two electrodes (A and B) and to measure the potential difference, ΔV (commonly measured in mV), by means of two other electrodes (M and N) on the surface of the earth, giving us a way to measure the electrical resistivity of the subsoil:

$$\Delta V_{MN} = I_{AB} \cdot \ R \tag{1}$$

where ΔV_{MN} is the measured voltage between electrodes M and N; I_{AB} is the injected current between electrodes A and B, and R is the resistance of the material, measured in Ω, through which the current flows. As far as the potential between M and N, the current introduced through A and B, and the electrode configuration are known, the resistivity of the ground can be determined. This is referred to as the 'apparent resistivity', ρ_a, expressed in Ω·m:

$$\rho_a = K_g \cdot V_{MN}/I_{AB} \tag{2}$$

where, K_g (in meters) is called the geometric factor which depends on electrode geometry (array) and can be calculated from the different electrodes spacing.

An inversion approach is applied to turn from the apparent resistivity to the true spatial distribution of the resistivity. The electrical resistivity tomography (ERT) is largely applied in shallow investigations to solve environmental, engineering and geological problems (e.g. Caputo et al. 2003; Lapenna et al. 2003; Chambers et al. 2006 and references therein). Continuous improvements in the field technology and data processing allow it to be one of the most employed geophysical methods for investigating the subsoil in the range of 0–200 m. Therefore, a new approach (investigating depths >500 m) was introduced for deep geological investigations. As described in Balasco et al. (2022), to increase the resolution for deeper targets (>500 m), it is necessary to improve the low S/N ratio in voltage recordings increasing the useful signal produced by the square wave of a DC injected into the ground. The main task of the DERT is the use of a dipole-dipole array configuration where the current injection dipole and the voltage acquisition dipole are physically separated. Beyond this technological solution, the peculiarity of the DERT is also the use of large electrode distances (>200 m) and generally long profiles (>3000 m) thus allowing to reach large investigation depths (>500 m).

In the specific case study of Ferrara city, the DERT was acquired with a deep multi-channel system designed and built at the Hydrogeosite Laboratory of the CNR-IMAA (Figure 6). This device enables the system to be expanded and adapted to various logistical conditions, allowing for the collection of a larger volume of data in a relatively short time, significantly reducing overall survey durations. In detail, long stainless-steel current electrodes (A and B) are connected to a transmitting station consisting of a transmitter Zonge GGT-10, a voltage regulator, and an external power system (ZMG-9). This energizing system can inject into the ground a time-domain

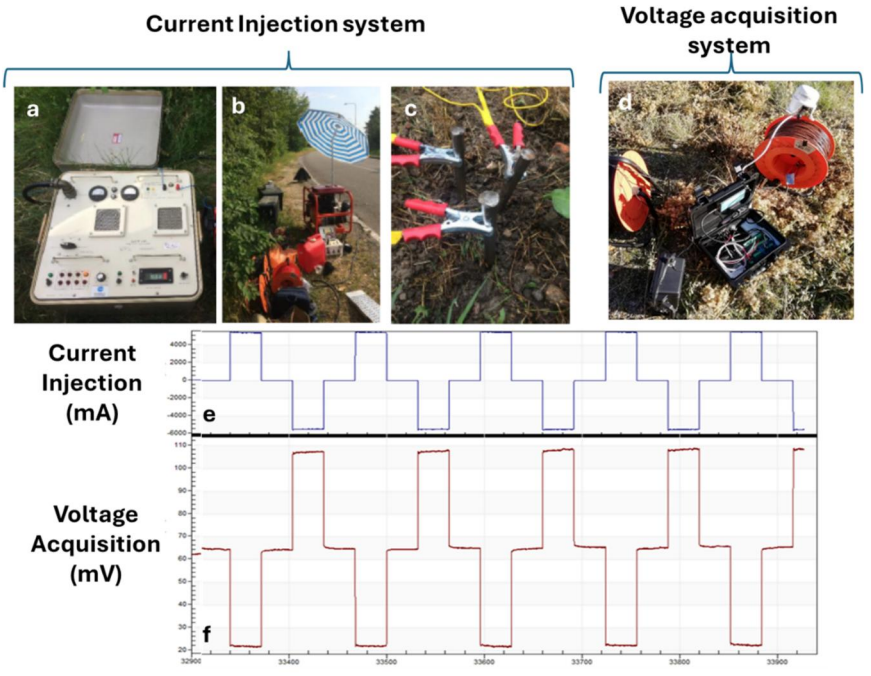

Figure 6. New DERT device system. Transmitter units (a) are connected with a power supply (b). The current is injected with a rose electrodes configuration (c) and the drop of potential is acquired with a data logger and cables connected with unpolarized electrodes. The current (e) and the drop of potential (f) are acquired in an automatic data logger.

(50% duty cycle) square-waveforms current signal of 32 sec, with a maximum energizing current of 20 A (Figure 6a–b).

The injected current is recorded in real time on the transmitter and to guarantee enough square wave recordings for signal analysis the injection time should last for at least 20 min for each current dipole. Furthermore, the voltage measuring system consists of stainless-steel potential electrodes (M and N) connected to a multichannel receiver system consisting of 6 remote multichannel dataloggers (Figure 6d), a GPS antenna and a radio connected to a personal computer. The system can simultaneously record a maximum of 8 generated voltage signals (mV) for each datalogger with a recording frequency of 100 Hz, together with timing and geographic position. The use of a long monopolar electric cable for connecting the electrodes at both transmitting and receiving stations allows a better management of the electrode positions and array configuration and particularly their large separation, up to more than 200 m.

In order to avoid polarization phenomena of potential electrodes, a dipole-dipole array configuration was used, where an electric current pulse (I) is sent into the ground *via* electrodes A and B, and the potential drop (ΔV) is measured between other two electrodes (M and N). In turn, M-N dipoles became energized dipoles when connected to the transmitter. During the survey, the A-B and M-N dipoles length ranged between 250 and 750 m, whereas the maximum dipole separation was of 3500 m. In total, 21 current injections have been performed and consequently

240 resistivity data, related to different current and potential electrode positions, were measured.

The data acquired in the field were processed through a procedure built ad hoc for this type of geoelectric surveys (DERT). In fact, electric potential and input current signals are recorded for over 20 min for each dipolar pair whose distance between transmitter and receiver can be up to several kilometres. Figure 6f shows an example of a recorded signal. In general, data quality decreases as a function of the distance between the receiver and the transmitter. In an urban environment like the one explored by the present research, this criticality could increase due to the presence of very high anthropogenic noise and therefore an off-line processing (post-acquisition) was performed by data analysis procedures both in the frequency domain (FFT) and in the time domain (stacking). At this regard, it is assumed that the voltage value $x(t)$ is composed of a periodic component, the signal $s(t)$, and a noisy component, $r(t)$:

$$x(t) = s(t) + r(t) \quad [3]$$

For the purpose of improving the results, a particular effort was spent in removing the noisy component from the measured voltage value, thus better resolving the amplitude of the signal, which represents the voltage value to be considered for the subsequent calculation of the resistivity. For this reason, an ad hoc approach has been applied allowing to filter the noise by means of an FFT analysis. As concerns the data acquired in the frame of this project, we applied the processing procedure represented in the diagram of Figure 7. The automatic processing consisted of synchronizing electric potential and current time series, filtering spikes and self-potential drifts, computing an FFT analysis on voltage and current signals for amplitude estimate, and calculating the resistance from the previous measurements considering Equation (1).

The 240 electrical resistivity data were obtained from the data analysis of more than 200.000 raw data. The voltage signal amplitude of the selected data ranges between 1 and 150 mV while the apparent resistivity of the data ranges from 1 to

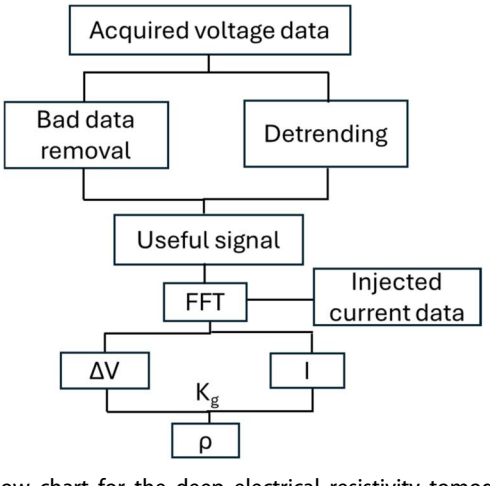

Figure 7. Data analysis flow chart for the deep electrical resistivity tomography, in order to determine the drop of potential with very low s/n ratio to determine the resistivity values.

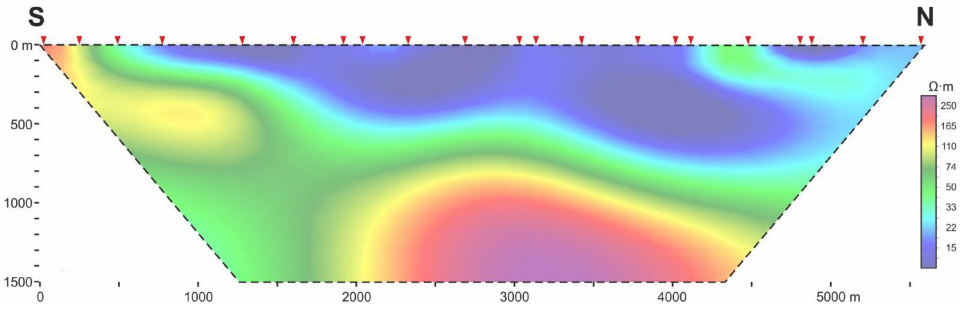

Figure 8. The inversion DERT results of the apparent electrical resistivity. See Figure 2 for location.

2300 Ω·m. The theoretical distribution of the data points that show a higher apparent resistivity are observed in the southern and deeper parts of the profile. The apparent resistivity data inversion was performed by ZondRes2D software (Zond geophysical software). It is a computer program for 2.5D interpretation of electrical resistivity datasets which uses a finite-element method to solve forward and inverse problems. The first step was to prepare the data for the inversion, such as poor data detection. The next step was to select the inversion type and parameters. To transform the apparent resistivity pseudo-section into a model representing the distribution of the calculated electrical resistivity in the subsurface, a smoothness constraint has been applied. The latter is a least-square inversion method based on a smoothing operator. The inversion type was Marquardt classic inversion algorithm consisting of a least-square method with regularization by a damping parameter (Marquardt 1963). In case of a small quantity of section parameters, this algorithm allows to definition the model of the subsurface heterogeneities (Figure 8). The starting model of the inversion consists of a 10 Ω·m homogeneous medium assuming triangular meshes with dimensions varying between 50 and 300 m. The final RSM was 2%.

4. Results

The depth-converted seismic reflection profile OGS1 (Figure 5) clearly shows the first major seismic reflectors ('a' in Figure 5b) between 150 and 250 m-depth, laterally continuous along the entire profile and with a sub-horizontal setting. Although much less continuous, also in the shallower portion of the profile reflectors seem to be sub horizontal. Similarly, sub horizontal reflectors could be also observed at 310–380 m-depth in the southernmost sector of the profile (CDPs 10–80; 'b' in Figure 5b), between 370 and 420 m along a large central portion (CDPs 110–390; 'c' in Figure 5b) and at 490–520 m in the northern part (CDPs 320–500; 'd' in Figure 5b).

Probably the most marked reflectors in terms of amplitude of the signal and lateral continuity across the entire profile is observed from 400–420 m-depth at the southern end (CDP 10), which progressively deepens to 580–600 m-depth at CDP 360-370 ('e' in Figure 5b). Further north, the same reflectors become sub horizontal or even slightly shallower, reaching 560–590 m-depth at CDP 500 ('f' in Figure 5b). A similar trend is described by a slightly deeper reflector starting at CDP 190 (550 m) and continuing to the northern end (CDP 500; 'g' in Figure 5b). Overall, these reflectors

define an almost 2 km-long (up to ca. CDP 370) monocline dipping 5° to 10° northwards, becoming sub horizontal or even gently southwards dipping, therefore defining a very open syncline. On top of this large-scale structure, it is worth to note that at the bottom of the previously described younger succession of sub horizontal reflectors, typical onlap geometries could be observed (red arrows in Figure 5b). Finally, in the deeper portion of the profile down to at least ca. 1500 m, several other reflectors could be observed all of them gently dipping northwards.

As concerns the results of the deep geoelectrical survey (DERT profile; Figure 8), the inverted image obtained on the basis of the collected data shows electrical resistivity values in the range 1–350 Ω·m, which are essentially compatible with the presence of sand, silt, clays, and marls of continental and marine successions. At a first glance, the resistivity distribution shows a downwards gradient, that is to say from more conductive to more resistant sediments; the gradient is not vertical, but strongly dipping southwards. In other terms, the resistivity isolines indicate a general northward dipping setting. In particular, the shallower portion of the tomography, reaching the surface at 300 m from the horizontal origin (south), and deepening to ca. 800 m at the end of the inverted profile (ca. 5000 m distance) is characterized by resistivity values lower than 20–30 Ω·m. Only exception is a minor shallow resistivity lens in the northern sector (4100–4500 m distance), that in any case shows values smaller than 40–45 Ω·m. As above mentioned, in the deeper portion of the profile roughly below the contour line of 50-60 Ω·m, resistivity values rapidly increase becoming >200 Ω·m. Such values are reached in the resistivity layer located at 700 m depth, between 2000 m from the origin to the end of the profile. On the contrary, in the southern sectors, this resistivity layer is discontinuous and much shallower, and with lower resistivity values (90–140 Ω·m).

In terms of geological and hydrogeological interpretation, the shallow conductivity zone (<20–30 Ω·m) should be correlated with the alluvial sediments characterized by silty-muddy deposits alternating with sandy lenses, like the shallow resistivity lens (4100–4500 m from the origin). The deep resistivity layer should be instead associated to the marly-to-clastic succession including the upper portion of the Scaglia Formations (Figure 3). Finally, the lateral discontinuity of the deep resistivity layer could been tentatively associated to a secondary tectonic feature representing an accommodation structure, which is not well defined in the seismic image (Figure 5) being shorter than the DERT profile.

5. Discussion

Notwithstanding the two deep geophysical surveys were based on substantially different and independent techniques, their results show large similarities. Taking into account the different resolutions and the different approaches for depth conversion applied to the two geophysical datasets, the two profiles have overlapped (Figure 9a). In particular, they both visibly show the presence of a shallow wedge being a few hundred meters thick in the southern sector, becoming 600–800 m-thick in the northern part. On the other hand, the seismic reflection profile OGS1 clearly shows a horizontal layering of this upper sedimentary succession and several onlap geometries at

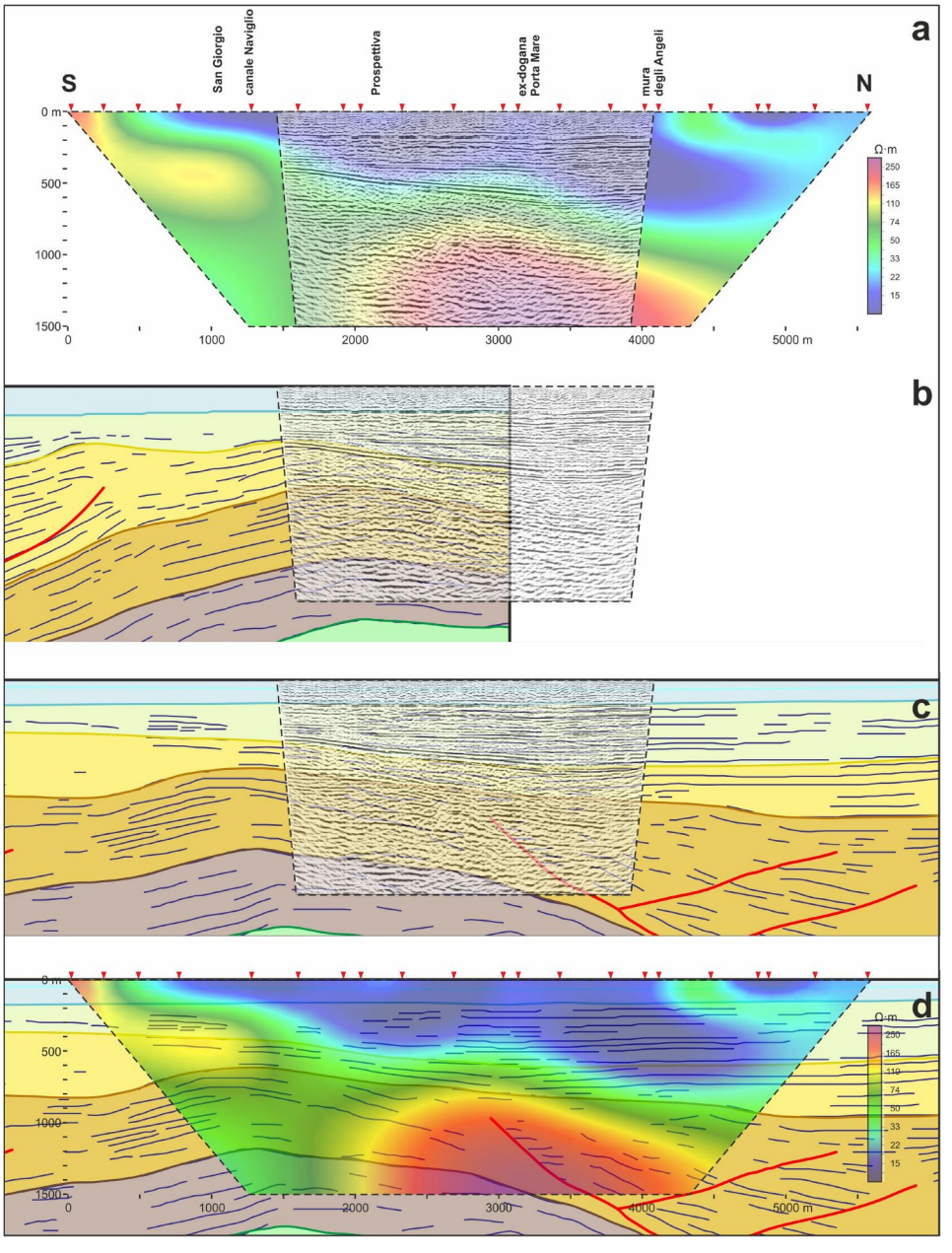

Figure 9. Comparison between the geophysical surveys carried out the in the frame of the present research (OGS1 and DERT) across the Eastern sector of the Ferrara urbanized area and the deep seismic reflection profiles for hydrocarbon exploration (BOL-20 and for-188).

the bottom. This sedimentary wedge seems to overly be a gently northward dipping monocline characterizing the lower portion of the profile down to the maximum investigated depth (ca. 1500 m).

We also compare our results with the ones based on deeper seismic reflection profiles (Figure 3). It is worth noting that our profile has been obtained in urban

conditions with all logistic limitations discussed in a previous section and at a relatively low cost, while the other ones have been carried out for hydrocarbon explorations, with expensive technologies and have been also calibrated with deep boreholes (e.g. Mistroni 2016; Mastella 2018).

For the purpose of this comparison, we projected the interpretation of the deep seismic profiles onto ours (Figure 9b-d) trying to account for the slight graphical distortion due to the imperfect parallelism of the traces (Figure 2). Considering also the distance of 500–1000 m for profile BOL-20 and 1500–3000 m for profile FOR-188, and consequently the possible lateral variations of the tectonic structures and the overall stratigraphy at depth, our OGS1 profile nicely reproduces the overall pattern of seismic reflectors, but especially it provides several additional details, due to its much higher quality and resolution, allowing to improve our view of the subsoil within the investigated transect. Indeed, the observed monocline represents the northern flank of a major anticline whose crest area is immediately south of the OGS1 (Figures 1 and 9b-c).

As previously described, on the northernmost sector of our seismic profile, the layering becomes sub-horizontal, therefore also confirming the northwards lateral transition to a large scale very gentle syncline (Figure 9c). Accordingly, the observed overlying wedge represents the laterally variable infilling of the Middle Pleistocene marine sedimentary unit (the so-called Gruppo di Asti; Figure 3) progressively sealing the Late Messinian-Early Pleistocene post-evaporitic deposits. The latter unit is markedly involved in a fault-propagation folding event, together with the Oligocene-Miocene units, as well as the mainly Palaeogene Scaglia Formations. On top, the relatively tabular and hence poorly deformed continental (Middle-)Late Quaternary unit.

Taking into account the difference in the overall number of measurements, in the characteristics of the geophysical recorded signal and interpolated parameters, and hence the different resolution that the electrical resistivity technique can provide, also between the DERT obtained in this research and the deep seismic reflection profiles there is an overall good agreement (Figure 9d). Indeed, the low-resistivity materials could be mainly associated with the Quaternary mostly clastic deposits, which are still characterized by a relatively high porosity and hence an important water content as an average. Moving downwards in the stratigraphic succession, firstly, depositional units are progressively more compacted hence similarly reducing their mean porosity and, secondly, the marly-carbonate component also increases in the older formations becoming dominant in the Oligocene-Miocene units. As a consequence, electrical resistivity should also progressively increase.

6. Concluding remarks

In conclusion, the 5600 m-long DERT and the 2630 m-long seismic reflection profile were carried out along the vallum between the sixteenth century walls and the modern eastern sector of the town (Figure 2). Analyses and interpretation allowed us to reconstruct the 'local' stratigraphic-depositional geometry until a depth of about 1.5 km, and to highlight the occurrence of a syndepositional Quaternary tectonic tilting associated to the growth of a fault-propagation fold. The obtained information on

the subsurface geology will be also crucial for the Ferrara Administration for updating and improving the territorial and urban planning tools for the mitigation of hydro-geological and seismic risks.

Acknowledgments

We are thankful to Lorella Dall'Olio (Ferrara Administration) for her contribution in the permission procedure to carry out the geophysical surveys. We also wish to remember Lorenzo Petronio who after leading the seismic reflection survey prematurely disappeared. He was a teacher for some of the authors and a friend for all of us. This paper is dedicated to his memory.

Authors' contributions

Conceptualization, E.R. and L.P.; methodology, E.R., L.P, and S.P.; soft-ware, A.A., E.R., L.B., L.P. and V.G.; validation, E.R. and L.P.; formal analysis, A.A., E.R., L.B. and V.G.; investigation, A.A., E.R., G.D, J.B., L.B., L.C., L.P. and S.P.; data curation, A.A., E.R. and L.P.; writing—original draft preparation, A.A., E.R., D.R. and R.C.; writing-review and editing, E.R., D.R. and R.C.; visualization, E.R., L.P.; supervision, E.R. and L.P.; project administration, L.P., R.C. and V.L.; funding acquisition, L.P., R.C. and V.L. All authors have read and agreed to the published version of the manuscript.

Disclosure statement

No potential conflict of interest was reported by the author(s).

Funding

Field work was funded by Italian MIUR in the frame of the CLARA Project 'Cloud Platform and smart underground imaging for natural risk assessment'. D.R. is supported by a contract in the frame of the PON REACT EU Project by the Italian MUR; number 09-G-48651-15.

Data availability statement

The data that support the findings of this study are available from E.R. and A.A., upon reasonable request.

References

Allegra Garufi R. 2016. Analisi di profili sismici per la ricostruzione del modello geologico tridimensionale ad est di Ferrara. MSc thesis, University of Ferrara, pp. 75 (unpublished)

Amorosi A, Pavesi M, Ricci Lucchi M, Sarti G, Piccin A. 2008. Climatic signature of cyclic fluvial architecture from the Quaternary of the central Po Plain, Italy. Sedim Geol. 209(1–4): 58–68. doi: 10.1016/j.sedgeo.2008.06.010.

Amorosi A, Bruno L, Campo B, Costagli B, Hong W, Picotti V, Vaiani SC. 2021. Deformation patterns of upper Quaternary strata and their relation to active tectonics, Po Basin, Italy. Sedimentol. 68(1):402–424. doi: 10.1111/sed.12784.

Arca S, Berretta GP. 1985. Prima sintesi geodetica-geologica sui movimenti verticali del suolo nell'Italia Settentrionale. Boll Geod Sci Aff. 44(2):125–156.

Balasco M, Lapenna V, Rizzo E, Telesca L. 2022. Deep electrical resistivity tomography for geophysical investigations: the state of the art and future directions. Geosciences. 12(12):438. doi: 10.3390/geosciences12120438.

Baradello L, Accaino F. 2013. Vibroseis deconvolution: a comparison of pre and post correlation vibroseis deconvolution data in real noisy data. J Appl Geophys. 92:50–56. doi: 10.1016/j.jappgeo.2013.02.009.

Bellanova J, Calamita G, Catapano I, Ciucci A, Cornacchia C, Gennarelli G, Giocoli A, Fisangher F, Ludeno G, Morelli G, et al. 2020. GPR and ERT investigations in urban areas: the case-study of Matera (Southern Italy). Rem. Sens. 12(11):1879. doi: 10.3390/rs12111879.

Berkhout AJ. 1977. Least-squares inverse filtering and wavelet deconvolution. Geophysics. 42(7):1369–1383. doi: 10.1190/1.1440798.

Bigi G, Bonardini G, Catalano R, Cosentino D, Lentini F, Parotto M, Sartori R, Scandone P, Turco E. 1992. Structural model of Italy, 1:500,000. Consiglio Nazionale delle Ricerche, Progetto Finalizzato Geodinamica, SELCa Firenze.

Bonini L, Toscani G, Seno S. 2014. Three-dimensional segmentation and different rupture behavior during the 2012 Emilia seismic sequence (Northern Italy). Tectonophys. 630:33–42. doi: 10.1016/j.tecto.2014.05.006.

Calamita G, Serlenga V, Stabile TA, Gallipoli MR, Bellanova J, Bonano M, Casu F, Vignola L, Piscitelli S, Perrone A. 2019. An integrated geophysical approach for urban underground characterization: the Avigliano town (southern Italy) case study. Geomatics Nat Hazards Risk. 10(1):412–432. doi: 10.1080/19475705.2018.1526220.

Capozzoli L, Capozzoli V, De Martino G, Duplouy A, Henning A, Rizzo E. 2023. The pre-Roman hilltop settlement of Monte Torretta di Pietragalla: first results of the geophysical survey. Archaeol Prosp. 30(1):33–46. doi: 10.1002/arp.1793.

Caputo M, Pieri L, Unguendoli M. 1970. Geometric investigations of the subsidence in the Po delta. Boll Geofis Teor Appl. 13(47):187–207.

Caputo R, Piscitelli S, Oliveto A, Rizzo E, Lapenna V. 2003. The use of electrical resistivity tomographies in active tectonics: examples from the Tyrnavos Basin, Greece. J Geodyn. 36(1–2):19–35. doi: 10.1016/S0264-3707(03)00036-X.

Caputo R, Poli ME, Minarelli L, Rapti D, Sboras S, Stefani M, Zanferrari A. 2016. Palaeoseismological evidence for the 1570 Ferrara earthquake, Italy. Tectonics. 35(6):1423–1445. doi: 10.1002/2016TC004238.

Caputo R, Tarabusi G. 2016. Il complesso sistema di sorgenti sismogeniche nell'area ferrarese e i loro effetti nella storia. Accademia delle Scienze di Ferrara, Atti, 93, p. 166–177. ISSN 0365–0464.

Carminati E, Martinelli G, Severi P. 2003. Influence of glacial cycles and tectonics on natural subsidence in the Po Plain (Northern Italy): Insights from 14C ages. Geochem Geophys Geosyst. 4(10):1–14. doi: 10.1029/2002GC000481.

Carrier A, Fischanger F, Gance J, Cocchiararo G, Morelli G, Lupi M. 2019. Deep electrical resistivity tomography for the prospection of low- to medium-enthalpy geothermal resources. Geophys J Int. 219(3):2056–2072. doi: 10.1093/gji/ggz411.

Castelli F, Cornacchia C, Gueli R, Lapenna V, Caputo R. 2019. Il Progetto CLARA: CLoud plAtform and smart underground imaging for natural risk assessment. Boll. Geofis. Teor. Appl. 60(suppl. 2):sIX–sXVI.

Cenni N, Viti M, Baldi P, Mantovani E, Bacchetti M, Vannucchi A. 2013. Present vertical movements in Central and Northern Italy from GPS data: possible role of natural and anthropogenic causes. J Geodyn. 71:74–85. doi: 10.1016/j.jog.2013.07.004.

Chambers JE, Kuras O, Meldrum PI, Ogilvy RD, Hollands J. 2006. Electrical resistivity tomography applied to geologic, hydrogeologic, and engineering investigations at a former waste-disposal site. Geophysics. 71(6):B231–B239. doi: 10.1190/1.2360184.

Colella A, Lapenna V, Rizzo E. 2004. High-resolution imaging of the High Agri Valley Basin (Southern Italy) with electrical resistivity tomography. Tectonophys. 386(1-2):29–40. doi: 10.1016/j.tecto.2004.03.017.

Cremaschi M, Nicosia C. 2010. Corso Porta Reno, Ferrara (Northern Italy): a study in the formation processes of urban deposits. Il Quaternario. 23(2bis):373–376.
Di Maio R, Mauriello P, Patella D, Petrillo Z, Piscitelli S, Siniscalchi A. 1998. Electric and electromagnetic outline of the Mount Somma-Vesuvius structural setting. J Volc Geoth Res. 82(1–4):219–238. doi: 10.1016/S0377-0273(97)00066-8.
Perez Flores MA, Treviño EG. 1997. Dipole-dipole resistivity imaging of the Ahuachapan-Chipilapa geothermal field, El Salvador Geothermics. 26(5–6):657–680. doi: 10.1016/S0375-6505(97)00015-1.
Gabàs A, Macau A, Benjumea B, Bellmunt F, Figueras S, Vilà M. 2014. Combination of geophysical methods to support urban geological mapping. Surv Geophys. 35(4):983–1002. doi: 10.1007/s10712-013-9248-9.
Gangone G, Gallipoli MR, Tragni N, Vignola L, Caputo R. 2023. Soil-building resonance effect in the urban area of Villa d'Agri (Southern Italy). Bull Earthquake Eng. 21(7):3273–3296. doi: 10.1007/s10518-023-01644-8.
Ghielmi M, Minervini M, Nini C, Rogledi S, Rossi M. 2013. Late miocene-middle pleistocene sequences in the Po Plain - Northern Adriatic Sea (Italy): the stratigraphic record of modification phases affecting a complex foreland basin. Mar Petrol Geol. 42:50–81. doi: 10.1016/j.marpetgeo.2012.11.007.
Giocoli A, Magrì C, Piscitelli S, Rizzo E, Siniscalchi A, Burrato P, Vannoli P, Basso C, Di Nocera S. 2008. Electrical resistivity tomography investigations in the Ufita Valley (southern Italy). Ann Geophys. 51(1):213–223. doi: 10.4401/ag-4443.
Goupillaud PL. 1974. Signal design in the vibroseis technique. SEG Geophysics Reprint Series. 11:152–165.
Govoni A, Marchetti A, De Gori P, Di Bona M, Lucente FP, Improta L, Chiarabba C, Nardi A, Margheriti L, Piana Agostinetti N, et al. 2014. The 2012 Emilia seismic sequence (Northern Italy): Imaging the thrust fault system by accurate aftershock location. Tectonophys. 622:44–55. doi: 10.1016/j.tecto.2014.02.013.
Guidoboni E. 1984. Riti di calamità: terremoti a Ferrara nel 1570-74. In: Caracciolo A. and Calvi G. editors), Calamità Paure Risposte, Quaderni storici, 55, p. 107–135.
Laing WE. 1972. Some basics and applications of the VIBROSEIS system of exploration. SPE Eastern Regional Meeting, SPE-4157-MS, 1972, 11, doi: 10.2118/4157-ms.
Laing WE. 1989. History and early development of the vibroseis system of seismic exploration: vibroseis. SEG Geophysics Reprint Series. 11:749–765.
Lapenna V, Lorenzo P, Perrone A, Piscitelli S, Sdao F, Rizzo E. 2003. High-resolution geoelectrical tomographies in the study of the Giarrossa landslide (Potenza, Basilicata). Bull Eng Geol Environ. 62(3):259–268. doi: 10.1007/s10064-002-0184-z.
Lapenna V. 2017. Resilient and sustainable cities of tomorrow: the role of applied geophysics. Boll. Geofis. Teor. Appl. 58:237–251. doi: 10.4430/bgta0204.
Liberty L. 2011. Hammer seismic reflection imaging in an urban environment. The Leading Edge. 30(2):146–153. doi: 10.1190/1.3555324.
Liu L, Chan LS. 2007. Sustainable urban development and geophysics. J Geophys Eng. 4(3):243–243. doi: 10.1088/1742-2140/4/3/E01.
Marquardt D. 1963. An algorithm for least-squares estimation of nonlinear parameters. SIAM J Appl Math. 11(2):431–441. doi: 10.1137/0111030.
Martí D, Carbonell R. 2016. Shallow seismic characterization in urban areas: challenges and solutions. In: Beer M., Kougioumtzoglou I., Patelli E. and Au I.K., editors. Encyclopedia of earthquake engineering. Berlin, Heidelberg: Springer. doi: 10.1007/978-3-642-36197-5_368-1.
Mastella G. 2018. Interpretazione di profili sismici per la ricostruzione di un modello geologico 3D del sottosuolo di Ferrara. BSc thesis, University of Ferrara, pp. 75 (unpublished)
Mistroni L. 2016. Interpretazione di un profile sismico attraverso l'Arco di Ferrara Centrale. BSc theis, University of Ferrara, pp. 58 (unpublished)
Molinari FC, Boldrini G, Severi P, Dugoni G, Rapti Caputo D, Martinelli G. 2007. Risorse idriche sotterranee della Provincia di Ferrara. In: Dugoni G. and Pignone R. Editors. Risorse

idriche sotterranee della Provincia di Ferrara. Regione Emilia Romagna, DB MAP Ed. 2007, Firenze 61 pp.
Morse PE, Hildebrandt GI. 1989. Ground roll suppression by the stalkarray. Geophysics. 54(3): 290–301. doi: 10.1190/1.1442654.
Olita F, Giampaolo V, Rizzo E, Palladino G, Capozzoli L, De Martino G, Prosser G. 2023. Investigation of the geological structure of the Tramutola Area (Agri Valley): inferences for the presence of geofluids at shallow crustal levels. Geosciences. 13(3):83. doi: 10.3390/geosciences13030083.
Papadopoulos N, Sarris A, Yi M-J, Kim J-H. 2009. Urban archaeological investigations using surface 3D ground penetrating radar and electrical resistivity tomography methods. Expl Geophys. 40(1), 56-68 doi: 10.1071/EG08107.
Patitucci Uggeri S. 1989. Castra' e l'insediamento sparso tra V e VIII secolo. In: Alfieri N. (Ed.), Storia di Ferrara, l'età antica (2.), 4. a. C.-6. d.C. Corbo G., Ferrara, p. 407–564.
Pezzo G, Merryman Boncori JP, Tolomei C, Salvi S, Atzori S, Antonioli A, Trasatti E, Novali F, Serpelloni E, Candela L, et al. 2013. Coseismic deformation and source modeling of the May 2012 Emilia (Northern Italy) Earthquakes. Seism Res Letts. 84(4):645–655. doi: 10.1785/0220120171.
Pieri M, Groppi G. 1981. Subsurface geological structure of the Po Plain, Italy. Consiglio Nazionale delle Ricerche, Progetto finalizzato Geodinamica, sottoprogetto Modello Strutturale, pubbl. N° 414, Roma. :23.
Pucci S, Civico R, Villani F, Ricci T, Delcher E, Finizola A, Sapia V, De Martini PM, Pantosti D, Barde-Cabusson S, et al. 2016. Deep electrical resistivity tomography along the tectonically active Middle Aterno Valley (2009 L'Aquila earthquake area, central Italy). Geophys J Int. 207(2):967–982. doi: 10.1093/gji/ggw308.
Rapti-Caputo D, Bratus A, Santarato G. 2009. Strategic groundwater resources in the Tagliamento River basin (Northern Italy): hydrogeological investigation integrated with geophysical exploration. Hydrogeol J. 17(6):1393–1409. doi: 10.1007/s10040-009-0459-6.
Rapti Caputo D. 2000. Groundwater resources east of Ferrara: investigations on hydrogeological and hydrochemical behaviour. Proposals for optimal management. Ph.D. Thesis, University of Ferrara, 215 pp. (in Italian)
Rapti Caputo D, Martinelli G. 2009. Geochemical and isotopic composition of the groundwater resources of the Po River delta (Northern Italy): implications for the environmental impact. Hydrogeol J. 17(2):467–480. doi: 10.1007/s10040-008-0370-6.
Rapti D, Caputo R. 2021. Environmental and energetic implications of the geothermal anomalies in the eastern Po Plain. It J Eng Geol Environ. 1:195–207. doi: 10.4408/IJEGE.2021-01.S-18.
Regione Emilia-Romagna and ENI-AGIP. 1998. Riserve idriche sotterranee della Regione Emilia-Romagna. In: Di Dio G. editor. Florence: S. El.Ca; p. 120.
Regione Lombardia and ENI-AGIP. 2002. Geologia degli acquiferi Padani della Regione Lombardia. Carcano C. and Piccin A. editors, Florence: S. El.Ca; p. 130.
Ricci Lucchi F, Colalongo ML, Cremonini G, Gasperi G, Iaccarino S, Papani G, Raffi I, Rio D. 1982. Evoluzione sedimentaria e paleogeografica del margine appenninico. In: Cremonini G. and Ricci Lucchi F. editors. Guida alla geologia del margine appenninico-padano. Guide Geologiche Regionali Soc Geol Ital., p. 17–46.
Rizzo E, Colella A, Lapenna V, Piscitelli S. 2004. High-resolution images of the fault-controlled High Agri Valley basin (Southern Italy) with deep and shallow electrical resistivity tomographies. Phys. Chem. Earth. 29(4-9):321–327. doi: 10.1016/j.pce.2003.12.002.
Rizzo E, Giampaolo V. 2019. New deep electrical resistivity tomography in the High Agri Valley basin (Basilicata, Southern Italy). Geomatics Nat Hazards Risk. 10(1):197–218. doi: 10.1080/19475705.2018.1520150.
Rizzo E, Piscitelli S, Bellanova J, Capozzoli L, De Martino G, Guerriero M, Morelli G, Fischanger F, Caputo R, Lapenna V. 2019a. Deep electrical resistivity tomography (DERT) for the geological-hydrogeological study of Ferrara. Bollettino di Geofisica Teorica ed Applicata. 60:100–105.

Rizzo E, Capozzoli L, De Martino G, Grimaldi S. 2019b. Urban geophysical approach to characterize the subsoil of the main square in San Benedetto del Tronto town (Italy). Eng Geol. 257:105133. doi: 10.1016/j.enggeo.2019.05.010.

Rizzo E, Giampaolo V, Capozzoli V, Grimaldi S. 2019c. Deep electrical resistivity tomography for the hydrogeological setting of Muro Lucano Mounts aquifer (Basilicata, Southern Italy). Geofluids. 2019:1–11. doi: 10.1155/2019/6594983.

Rizzo E, Giampaolo V, Capozzoli L, De Martino G, Romano G, Santilano A, Manzella A. 2022. 3D deep geoelectrical exploration in the Larderello geothermal sites (Italy). Phys Earth Planet Int. 329-330:106906. doi: 10.1016/j.pepi.2022.106906.

Sapia V, Villani F, Fischanger F, Lupi M, Baccheschi P, Pantosti D, Pucci S, Civico R, Sciarra A, Smedile A, et al. 2021. 3-D deep electrical resistivity tomography of the major basin related to the 2016 Mw 6.5 Central Italy earthquake fault. Tectonics. 40(4):e2020TC006628. doi: 10.1029/2020TC006628.

Sato H, Fehler MC, Maeda T. 2012. Seismic wave propagation and scattering in the heterogeneous earth: second Edition. New York: AIP Press/Springer, doi: 10.1007/978-3-642-23029-5.

Savit CH, Brustad JT, Sider J. 1958. The moveout filter. Geophysics. 23(1):1–25. doi: 10.1190/1.1438447.

Severi P. 2021. Soil uplift in the Emilia-Romagna plain (Italy) by satellite radar interferometry. Bull. Geophys. Ocean. 62(3):527–542. doi: 10.4430/bgta0349.

Steeples DW. 1998. Shallow seismic reflection section – Introduction. Geophysics. 63(4):1210–1212. doi: 10.1190/1.1444421.

Storz H., Storz W. and Jacobs F. (2000): Electrical resistivity tomography to investigate geological structures of the earth's upper crust. Geophys Prosp, 48(3). 455–471. doi: 10.1046/j.1365-2478.2000.00196.x.

Suzuki K, Toda S, Kusunoki K, Fujimitsu Y, Mogi T, Jomori A. 2000. Case studies of electrical and electromagnetic methods applied to mapping active faults beneath the thick Quaternary. Eng Geol. 56(1-2):29–45. doi: 10.1016/S0013-7952(99)00132-5.

Toscani G, Burrato P, Di Bucci D, Seno S, Valensise G. 2009. Plio-quaternary tectonic evolution of the northern Apennines thrust fronts (Bologna-Ferrara section, Italy.): Seismotectonic Implications. Boll Soc Geol It. 128(2):605–613. doi: 10.3301/IJG.2009.128.2.605.

Tragni N, Calamita G, Lastilla L, Belloni V, Ravanelli R, Lupo M, Salvia V, Gallipoli MR. 2021. sharing soil and building geophysical data for seismic characterization of cities using CLARA WebGIS: a case study of Matera (Southern Italy). Appl Sci. 11(9):4254. doi: 10.3390/app11094254.

Troiano A, Isaia R, Di Giuseppe MG, Tramparulo FDA, Vitale S. 2019. Deep electrical resistivity tomography for a 3D picture of the most active sector of Campi Flegrei caldera. Sci Rep. 9(1):15124. doi: 10.1038/s41598-019-51568-0.

Uggeri G. 1989. Insediamenti, viabilità e commerci di età romana nel ferrarese. In: Alfieri N. (Ed.), Storia di Ferrara, l'età antica (1.), 4. secolo a.C.-6. Secolo d.C. Corbo G., Ferrara, p. 1–209.

United Nations. 2019. Department of Economic and Social Affairs, Population Division (2019). World Urbanization Prospects: the 2018 Revision (ST/ESA/SER.A/420). New York: United Nations.

United Nations. 2020. Human Settlements Programme (UN-Habitat), 'Opinion: COVID-19 demonstrates urgent need for cities to prepare for pandemics'. 15 June 2020 Policy Brief: COVID-19 in an Urban World July 2020.

Valenti C. 2015. Caratterizzazione tettonico di un segmento dell'Arco Ferrarese mediante analisi di profili sismici. MSc thesis, University of Ferrara, pp. 55 (unpublished)

Vannoli P, Burrato P, Valensise G. 2015. The seismotectonics of the Po Plain (Northern Italy): tectonic diversity in a blind faulting domain. Pure Appl Geophys. 172(5):1105–1142. doi: 10.1007/s00024-014-0873-0.

Vincent PD, Tsoflias GP, Steeples DW, Sloan SD. 2006. Fixed-source and fixed-receiver walk-away seismic noise tests: a field comparison. Geophysics. 71(6):W41–W44. doi: 10.1190/1.2337573.

Yilmaz Ö. 2001. Seismic data analysis: processing, inversion, and interpretation of seismic data. (2001), "Front Matter," *Investigations in Geophysics* : i-xxiv., Editor Society of Exploration Geophysicists, Tulsa, OK 74170–2740 doi: 10.1190/1.9781560801580.